MITSUBISHI ELECTRIC RESEARCH LABORATORIES
https://www.merl.com

Inverse Design of Nanophotonic Devices using Deep Neural Networks

Kojima, Keisuke; Tang, Yingheng; Koike-Akino, Toshiaki; Wang, Ye; Jha, Devesh K.; Parsons, Kieran; TaherSima, Mohammad; Sang, Fengqiao; Klamkin, Jonathan; Qi, Minghao

TR2020-130 September 30, 2020

Abstract

We present three different approaches to apply deep learning to inverse design for nanophotonic devices. The forward and inverse regression models use device parameters as inputs and device responses as outputs, and vice versa. The generative model to create a series of improved designs. We demonstrate them to design nanophotonic power splitters with multiple splitting ratios.

Asia Communications and Photonics Conference (ACP)

© 2020 MERL. This work may not be copied or reproduced in whole or in part for any commercial purpose. Permission to copy in whole or in part without payment of fee is granted for nonprofit educational and research purposes provided that all such whole or partial copies include the following: a notice that such copying is by permission of Mitsubishi Electric Research Laboratories, Inc.; an acknowledgment of the authors and individual contributions to the work; and all applicable portions of the copyright notice. Copying, reproduction, or republishing for any other purpose shall require a license with payment of fee to Mitsubishi Electric Research Laboratories, Inc. All rights reserved.

Mitsubishi Electric Research Laboratories, Inc.
201 Broadway, Cambridge, Massachusetts 02139

Inverse Design of Nanophotonic Devices using Deep Neural Networks

Keisuke Kojima[1,2,*], Yingheng Tang[1,3], Toshiaki Koike-Akino[1], Ye Wang[1], Devesh Jha[1], Kieran Parsons[1], Mohammad H. Tahersima[1], Fengqiao Sang[2], Jonathan Klamkin[2], and Minghao Qi[3]

[1]*Mitsubishi Electric Research Laboratories (MERL), 201 Broadway, Cambridge, MA 02139, USA.*
[2]*Electrical and Computer Engineering Dept., University of California, Santa Barbara, CA, USA*
[3]*Electrical and Computer Engineering Dept., Purdue University, West Lafeyette, IN, USA*
**kojima @ merl.com*

OCIS codes: 250.5300, 160.3918, 100.4996.

Abstract: We present three different approaches to apply deep learning to inverse design for nanophotonic devices. The forward and inverse regression models use device parameters as inputs and device responses as outputs, and vice versa. The generative model to create a series of improved designs. We demonstrate them to design nanophotonic power splitters with multiple splitting ratios. © 2020 The Author(s)

1. Introduction

Application of neural networks (NNs) to improve the automation of photonic device design has recently drawn increased attention. In this paper, we show three major categories. First, we show an example of a deep neural network (DNN) used as a forward regression model. A NN based forward modeling in conjunction with an optimization method has been used for designing nanophotonic power splitters [1,2], nanophotonic mode converters [3], and optical attenuators [4]. Second, we show an inverse regression model [2,5] for designing nanophotonic power splitters [2, 5]. Next, we show an example of a DNN used as a generative model, which produces a set of new designs which can satisfy the target performance better. Generative models have been recently used for designing materials [6] and plasmonic devices [7, 8]. Here, we introduce a novel conditional variational autoencoder (CVAE) [9] combined with an adversarial network [10]. This is applied to a multi-level nanostructured device design, which can be a more complex optimization problem compared to a binary nanostructured device design, and can benefit from more sophisticated design algorithms.

2. Forward and Inverse Regression Models

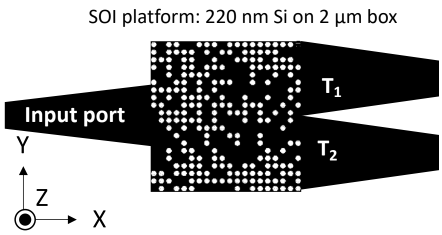

Fig. 1: Nanophotonic power splitter.

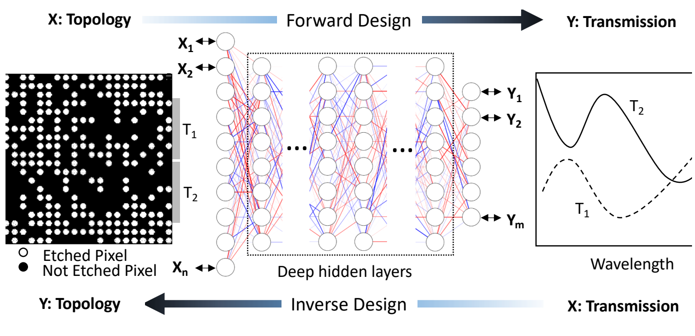

Fig. 2: DNNs for forward and inverse regression modeling [5]

The target device for our design/optimization is shown in Fig. 1, where 220nm-thick, 2.25μm wide square silicon-on-insulator (SOI) is used as the power splitter where 77.4 nm-diameter holes with 111.8 nm spacing are arranged to split and guide the light. Fig. 2 shows the concept of the regression model, where the network takes device topology design as input and spectral response of the metadevice as label or vice versa. In the first example, we use a DNN in the forward design model. Since the nanophotonic and photonic crystal design are analogous to image processing and recognition problems, we use convolutional neural networks (CNN) to improve the forward prediction accuracy [11].

Fig. 3 shows a comparison of a standard direct binary search (DBS) and DNN-assisted DBS. The latter compares 400 possible positions to flip using DNN before conducting each 3D finite-difference time-domain (FDTD) simulation. Here, we plotted a metric defined as

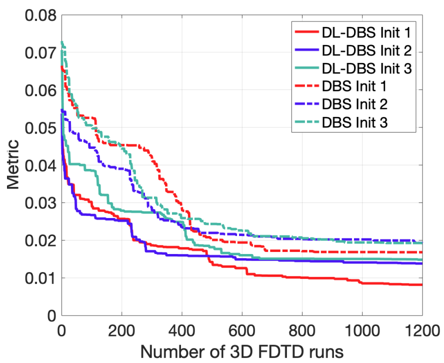

Fig. 3: Metric as a function of the number of 3D FDTD runs, for the conventional DBS and the DNN-DBS methods. Three different initial conditions are used [2].

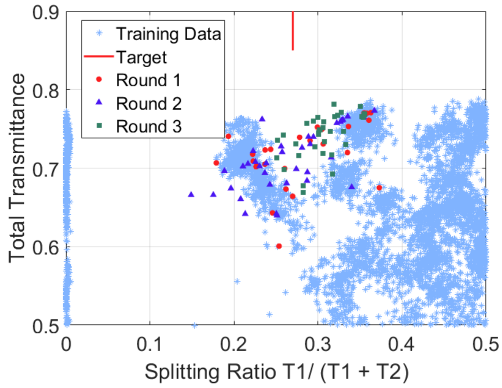

Fig. 4: Demonstration of inverse design for a power splitter with a splitting ratio of 0.27. Each marker denote the total transmittance is plotted against the splitting ratio. The red line denotes the target splitting ratio of 0.27 [2].

$$\text{Metric} = [|T_1 - T_1^{\star}|^2 + |T_2 - T_2^{\star}|^2 + \alpha \times R^2], \quad (1)$$

where T_1 and T_2 are the lowest transmitted power within the spectral range of 1300 nm and 1800 nm. $T_1^{\star} = 0.27$ and $T_2^{\star} = 0.73$ are used as an example target. We chose $\alpha = 10$ as a weighting factor to suppress reflection. The training data do not include any devices with the splitting ratio between 0.23 and 0.33, where the splitting ratio is defined as $T_1/(T_1 + T_2)$. It can be seen that DNN-assisted DBS optimizes the device structure much faster than the conventional DBS, especially at the early part of the optimization.

Alternatively, a DNN can be used in the inverse regression mode as shown in the bottom of Fig. 2 [5]. Here, we train the DNN using spectral responses as inputs, and device topology as outputs. Then a series of slightly different target spectral responses are given as inputs, and we obtain a set of improved results. This process can be repeated including the improved designs in the training data as shown in Fig. 4 [2].

3. Generative Deep Learning Model

In order to generate a series of improved designs from existing sub-optimal designs, we constructed a new generative deep learning model based on a CVAE [7, 9] and an adversarial block [8, 10] as shown in Fig. 5 [12, 13]. The device structure is similar to the one described in Section 2, We first use a variational autoencoder and convolutional layers to encode the original 20×20 data (HV: hole vector) to 60 latent variables which are the mean (μ) and co-variance (σ) of the normal distribution. Then we concatenate the transmission information to the latent variables and pass into the decoder. The purpose of the adversarial block is to make the encoder only extract the pattern information rather than the performance information. The generated pattern gives the Bernoulli's distribution at each location point and different hole sizes are used to represent such probability of the appearance of etched holes at certain locations.

To measure the performance of the generated devices, we use the following figure of merit (FOM):

$$\text{FOM} = 1 - 10 \times \left[\int_a^b |T_1(\lambda) - T_1^{\star}(\lambda)|^2 d\lambda + \int_a^b |T_2(\lambda) - T_2^{\star}(\lambda)|^2 d\lambda + \int_a^b \alpha \times R^2(\lambda) d\lambda \right], \quad (2)$$

where $T_1(\lambda)$, $T_2(\lambda)$, $R(\lambda)$, and $[\cdot]^{\star}$ denote transmissions of output ports 1 and 2, reflection at input port at certain wavelengths, and corresponding target values, respectively. Here, we used a wavelength range of $a = 1250$ nm and $b = 1800$ nm. Figure 6 shows the FOM of the generated devices as a function of the splitting ratio. Each star indicates generated data using the CVAE model, while open circles show data using the Adversarial-VAE model. Each color represents different target splitting ratio. The results show that for each targeting splitting ratio, the A-CVAE model generates improved FOM. The generated patterns, beam propagation, T_1, T_2, and $T_1 + T_2$ spectra are shown in Fig. 7.

References

1. K. Kojima, B. Wang, U. Kamilov, T. Koike-Akino, and K. Parsons, in *Integrated Photonics Research, Silicon and Nanophotonics,* (Optical Society of America, 2017), pp. ITu1A–4.
2. K. Kojima, M. H. Tahersima, T. Koike-Akino, D. Jha, Y. Tang, Y. Wang, and K. Parsons, invited, submitted for publication .

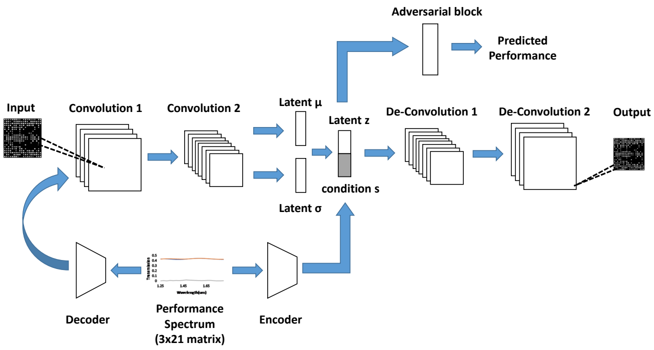

Fig. 5: CVAE structure with an adversarial block. Device structures are supplied as input/output conditions, and performance data are supplied as both latent condition and input condition [13].

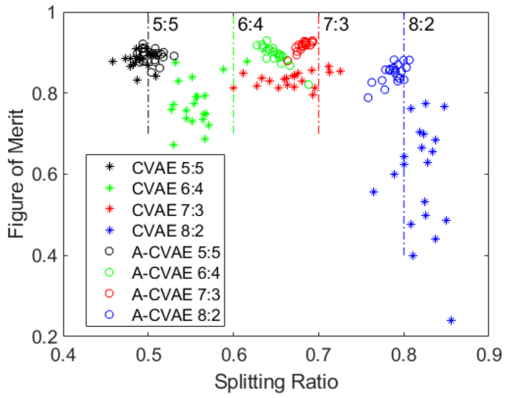

Fig. 6: FOM versus splitting ratio. Each color corresponds to different target splitting ratios [13].

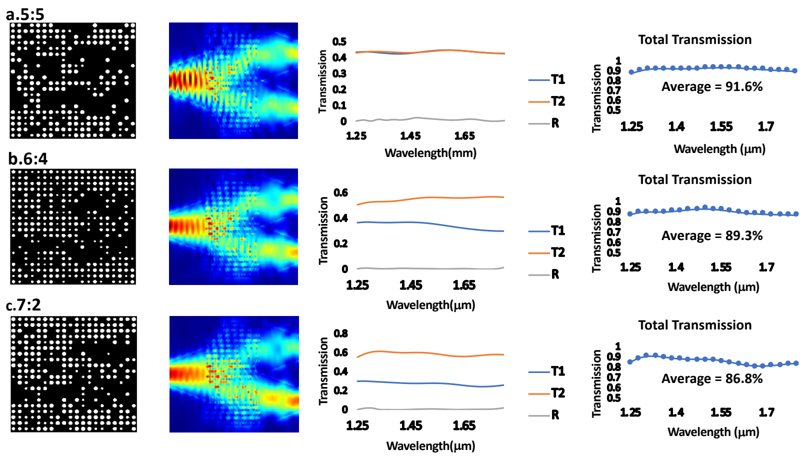

Fig. 7: (from left to right) The hole-in-Si-slab pattern generated from the adversarial CVAE model, transverse electric field (or intensity) profile, the FDTD simulated transmission spectra of the two output ports (T1 and T2) and reflection (R), and the total transmission spectra. Results for power splitting ratios of 5:5, 6:4, and 7:3 from top to bottom [13].

3. M. Teng, K. Kojima, T. Koike-Akino, B. Wang, C. Lin, and K. Parsons, in *2018 Optical Fiber Communications Conference and Exposition (OFC),* (2018), pp. 1–3.
4. Z. Chu, Y. Liu, J. Sheng, L. Wang, J. Du, and K. Xu, in *2018 Asia Communications and Photonics Conference (ACP),* (IEEE, 2018), pp. 1–3.
5. M. H. Tahersima, K. Kojima, T. Koike-Akino, D. Jha, B. Wang, C. Lin, and K. Parsons, Sci. Reports **9**, 1368 (2019).
6. B. Sanchez-Lengeling and A. Aspuru-Guzik, Science **361**, 360–365 (2018).
7. W. Ma, F. Cheng, and Y. Liu, ACS Nano **12**, 6326–6334 (2018).
8. Z. Liu, D. Zhu, S. P. Rodrigues, K.-T. Lee, and W. Cai, Nano letters **18**, 6570–6576 (2018).
9. K. Sohn, H. Lee, and X. Yan, in *Advances in neural information processing systems,* (2015), pp. 3483–3491.
10. I. Goodfellow, J. Pouget-Abadie, M. Mirza, B. Xu, D. Warde-Farley, S. Ozair, A. Courville, and Y. Bengio, in *Advances in neural information processing systems,* (2014).
11. M. H. Tahersima, K. Kojima, T. Koike-Akino, D. Jha, B. Wang, C. Lin, and K. Parsons, "Nanostructured photonic power splitter design via convolutional neural networks," in *CLEO: Science and Innovations,* (Optical Society of America, 2019), pp. SW4J–6.
12. O. Özdenizci, Y. Wang, T. Koike-Akino, and D. Erdoğmuş, in *2019 9th International IEEE/EMBS Conference on Neural Engineering (NER),* (IEEE, 2019), pp. 207–210.
13. Y. Tang, K. Kojima, T. Koike-Akino, Y. Wang, P. Wu, M. H. Tahersima, D. Jha, K. Parsons, and M. Qi, in *2020 Optical Fiber Communications Conference and Exhibition (OFC),* (2020), p. Th1A.1.